Heterodyne and direct detection wind lidar developed at ONERA

David Michel, Béatrice Augere, Thibault Bouland, Nicolas Cézard, Agnès Dolfi-Bouteyre, Anne Durecu, Didier Goular, François Gustave, Anasthase Liméry, Laurent Lombard, et al.

Heterodyne and direct detection wind lidar developed at ONERA

1st David Michel
ONERA
Palaiseau, France
david-tomline.michel@onera.fr

2nd Béatrice Augère
ONERA
Palaiseau, France
beatrice.augere@onera.fr

3rd Thibault Boulant
ONERA
Palaiseau, France
thibault.boulant@onera.fr

4th Nicolas Cézard
ONERA
Palaiseau, France
nicolas.cezard@onera.fr

5th Agnès Dolfi-Bouteyre
ONERA
Palaiseau, France
agnes.dolfi-bouteyre@onera.fr

6th Anne Durécu
ONERA
Palaiseau, France
anne.durecu@onera.fr

7th Didier Goular
ONERA
Palaiseau, France
didier.goular@onera.fr

8th François Gustave
ONERA
Palaiseau, France
francois.gustave@onera.fr

9th Anasthase Limery
ONERA
Palaiseau, France
anasthase.limery@onera.fr

10th Laurent Lombard
ONERA
Palaiseau, France
laurent.lombard@onera.fr

11th Jean-François Mariscal
LATMOS
Guyancourt, France
jean-francois.mariscal@latmos.ipsl.fr

12th Christophe Planchat
ONERA
Palaiseau, France
christophe.planchat@onera.fr

13th Jonathan Pouillaude
ONERA
Palaiseau, France
jonathan.pouillaude@onera.fr

14th Nicolas Rouanet
LATMOS
Guyancourt, France
nicolas.rouanet@latmos.ipsl.fr

15th Pierre Pichon
ONERA
Palaiseau, France
pierre.pichon@onera.fr

16th Matthieu Valla
ONERA
Palaiseau, France
matthieu.valla@onera.fr

***Abstract*—In this paper, we present the two wind lidar architectures developed at ONERA: the heterodyne lidar which analyzes the backscattering of particles and the direct detection lidar using a QMZ which analyzes the backscattering of molecules. In both cases, solutions have been developed to be able to embark them on an airplane: fiber laser, robust receiver, robust general architecture. Both technologies could provide interesting comparative measurements for AEOLUS calibration/validation campaigns: the heterodyne configuration allows precise measurements on the lower part of the atmosphere while the QMZ configuration allows reaching up to at an altitude of 20 km. In addition, regarding the developments made for molecular lidar, the UV fiber laser and the monolithic QMZ receiver could be excellent solutions for the next generation of Aeolus to reduce costs, improve data quality and lidar durability.**

***Index Terms*—UV Lidar, heterodyne Lidar, cal/Val, AEOLUS**

I. Introduction

The measurement of the wind by atmospheric lidar on board aircraft has many applications such as reducing the consumption of aircraft [1]–[4], aiding navigation for aircraft [5] or high-altitude platform systems [6], ...}, improving weather forecasts using wind measurements from space {future ADM-Aeolus lidar [7] or lidar calibration/validation}. The ADM-Aeolus mission was successfully launched in 2018 providing the first global wind profiles from space across the entire troposphere and lower stratosphere which led to a significant improvement in the weather forecast score [8]. A wind lidar emits a pulse through the atmosphere to determine, with a spectral analyzer, the wind speed projected on the axis of the lidar from the frequency shift of the backscattered light induced by the movement of particles and molecules due to of the Doppler effect. To achieve the 2 m/s velocity measurement accuracy required for AEOLUS over a wide velocity range, the mission places high demands on instrument performance, alignment stability, etc. In order to verify the overall performance, comparative measurements should be performed, especially with other wind lidar. In this respect, the use of onboard lidar makes it possible to follow the measurements made by the satellite and to bring the lidar to high altitude in order to improve the precision of the measurement. On the other hand, optimizing the technologies used to design Aeolus could lead to better performance, in particular better precision, greater longevity or lower weight, which would lead to a reduction in the overall cost of the mission and/or further improve the weather forecast score. For these two reasons, the exploration of new lidar technologies is very important for the mission and the continuation of AEOLUS.

This work was supported by the HORIZON EUROPE FRAMEWORK PROGRAMME [Call Reference N° : HORIZON-JU-Clean Aviation-2022-01]; l'Etat, le Ministère de la Transition écologique [Conventions N° 2021-37; N° 2020-28]

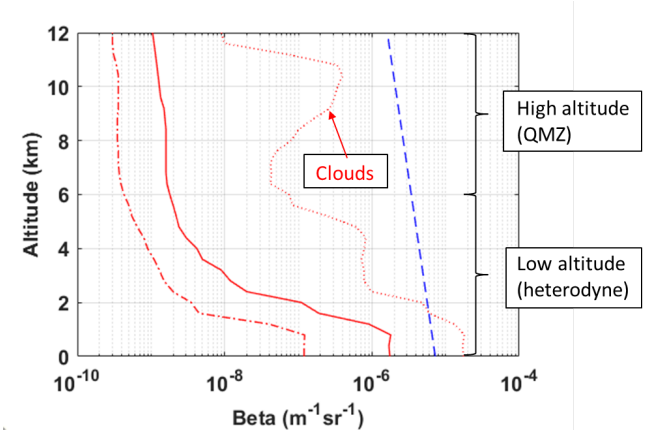

Fig. 1. Comparison of the evolution of the backscattering coefficient (Beta) as a function of altitude induced by molecules (dotted blue curve) and particles (red curves). For the particles, the curves correspond to threshold values valid for 10% (dotted curve), 50% (solid curve) and 90% (dotted-dotted curve) time.

Calibration/validation campaigns were carried out using several technologies including heterodyne particle lidar [9], [10], direct detection lidar optimized for particles [11] and molecules [12], [13]. Particle lidars that use Mie scattering are generally more mature, compact and give a more accurate measurement of wind speed. However, they are limited to the lower part of the atmosphere where the presence of particles is high enough to obtain measurements (Fig. 1) and the measurement area is very random because the presence of particles varies considerably depending on location and of time. Validations of AEOLUS measurements up to 8 km altitude for the 2 μm DLR lidar and up to 12 km altitude for the DAWN lidar were obtained with errors lower than 1 m/s . It can be noted that in both cases the heterodyne lidars include free space amplifiers to reach very high energies per pulse of 1-2 mJ for the DLR laser and 100 mJ for the DAWN lidar. On the other hand, the direct detection lidar optimized for the Rayleigh scattering of molecules allowed continuous comparisons up to 10 km altitude with the A2D DLR lidar and up to 30 km altitude with both the ground-based OHP lidar and OPAR lidar with wind measurement errors of $\sim$ 3 m/s and $\sim$ 1 m/s respectively. We can also mention that for these two case campaigns, the lasers used were very energetic with pulse energies of 60 mJ at 355 nm in the first case and 800 mJ at 532 nm in the second case. It can be noted that the laser wavelengths used for molecular lidar are low because the backscattering coefficient for Rayleigh backscattering is proportional to $1/\lambda^4$.

Although early studies considered using a heterodyne particle lidar for measurements from a satellite [14], [15], a direct detection lidar sensitive to Rayleigh scattering from molecules was chosen for ADM -Aeolus, called ALADIN, in order to obtain data up to 16 km altitude. To maximize molecular backscatter and limit eye safety issues, UV wavelength was used. The laser developed is a diode-pumped solid-state laser capable of achieving a repetition rate of 50 Hz and high pulse energies of $\sim$ 60 mJ. However, solid-state lasers have several disadvantages including high cost, weight, sensitivity to vibrations and the impossibility of operating in a vacuum because UV lasers damage optical surfaces. This last point notably forced the continuous injection of oxygen into the AEOLUS laser. These difficulties led to laser developments that took more than 10 years and to a significant delay in the launch date of the satellite. A significant drop in the energy also happened for the first laser after only about a year of operation, which led to a switch to the replacement laser. With regard to reception, the spectral analyzer which was chosen consists of an arrangement of two Fabry-Perrault interferometers which provide two channels positioned on either side of the molecular spectrum. when the molecular spectrum is shifted due to the wind speed, the signal on one channel increases while the other decreases, which makes it possible to quantify the frequency shift and therefore the wind speed. However, this method has several inherent drawbacks, including sensitivity to molecular spectral shape (thus temperature and pressure along the lidar axis) [16], [17], sensitivity to particulate scattering (requiring thus corrections with backscatter ratio measurements) [18], [19], is sensitive to lidar alignment due to its narrow field of view and requires high spectral stability.

In this paper, we present the developments made at ONERA on the particulate heterodyne lidar and the molecular direct detection lidar for on-board applications and discuss about potential applications for spatial agencies. After a description of the two measurement methods, we present typical performance simulations (for typical cal/val configurations). We describe then the various developments that have been made to make the two architectures more robust for use on an air carrier. Developments include the production of fiber lasers, compact receivers and robust optical analyzers. We finish by discussing the possible applications of ONERA lidar for AEOLUS calibration/validation campaigns and the use of developments made on the UV lidar for a future design of AEOLUS.

II. Measurement methods

The diagram of a wind lidar is presented in Fig. 2a). A pulsed laser of frequency f_{laser} is sent into the atmosphere. A small fraction of the laser is backscattered by particles and molecules with a frequency shift (Δf) proportional to the projection of their velocity ($\vec{V_{wind}} \rightarrow V_p$) on the lidar axis (Doppler effect) . This light ($f_{laser} + \Delta f$) is collected and a spectral analyzer is used to measure this offset and deduce the projected wind speed. The measurement is time-resolved to obtain spatial resolution because the light scattered at a distance z arrives at the detector at an instant $2z/c$ where c is the speed of light. Two methods have been developed at ONERA to perform frequency analysis:

- heterodyne detection used to measure wind speed from particulate backscatter
- High spectral resolution analyzer using a quadri Mach-Zehnder interferometer optimized to measure wind speed

from molecular backscatter (particles also contribute to the signal)

Both methods are described in this section and simulations of performances are presented.

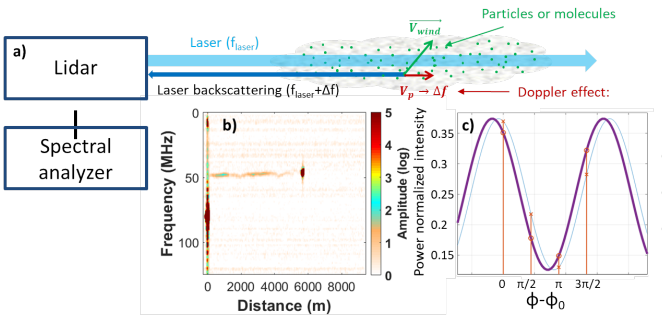

Fig. 2. a) Diagram of a wind lidar: a laser is sent into the atmosphere, the small fraction backscattered by the particles and molecules is collected and analyzed to determine the Doppler shift induced by the speed of the particles and molecules in order to deduce the wind speed. To analyze particle backscatter, we use heterodyne detection and compute the spectrogram (b) to determine the frequency shift and hence the wind speed at each distance. To analyze molecular backscattering, we use a quadri-Mach Zehnder interferometer which produces an interference state whose phase is proportional to the input optical frequency. The phase output is obtained from the four interference states (orange lines) in quadrature approximated by a sinusoid. The frequency shift is then deduced by comparing the phase of this sinusoid for the backscattered signal (blue curve) with the reference phase obtained with a laser sample (purple curve).

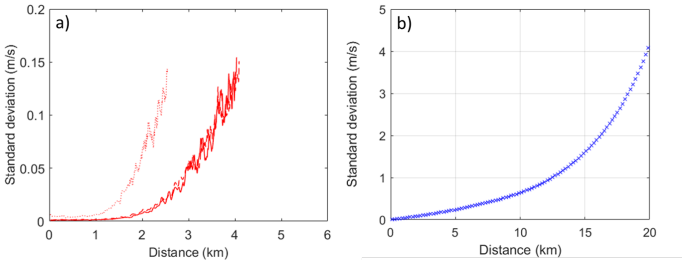

Fig. 3. Simulated standard deviation of the velocity measured by the LIVE lidar (a) and the QMZ molecular lidar (b) as a function of altitude for an instrument located on the ground and addressed upwards. In a), the values of beta correspond to the threshold values of Fig. 1 encountered 10% of the time (solid curve), 50% of the time (dotted curve) and 90% of the time (dotted curve). We can notice that the 2 last curves are very similar. This is due to the stronger laser absorption at low altitudes for the last curve that counterbalance the stronger backscattering coefficient after 2 km.

A. Heterodyne detection for particulate backscattering

Heterodyne detection consists of mixing a small fraction of the laser light with the backscattered light on the detector. This mixing leads to a heterodyne current which has a frequency equal to the frequency difference between the two waves (proportional to the wind speed). This current is acquired and digitized to obtain the heterodyne signal. Then, signal processing is performed to determine its time-resolved frequency. This processing is generally carried out by first calculating all the spectra where each spectrum is obtained for the heterodyne signal multiplied by a time window centered at a time t. This isolates the signal from a region around $z = ct/2$ where c is the speed of light. Fig. 2 b) shows an example of a spectrogram which corresponds to all the concatenated spectra presented as a function of z. Then, the maxima of the spectra are determined to measure the frequency shift and infer the spatially resolved wind speed. This method is not used for molecular scattering mainly because the Brownian motion of the molecules induces a spectral broadening of the heterodyne signal much larger than the bandwidth of the detectors. To present the properties of the heterodyne lidar developed at ONERA and to underline the high precision that can be obtained on the wind measurement with such an instrument, we carried out a simulation of the 1.5 μm lidar LIVE (LIdar VEnt) [20] when the instrument is on the ground and facing upwards [Fig. 3a)]. This monostatic lidar (i.e. the same optics are used to spatially shape the laser and to collect the signal) uses a laser with a repetition rate of 14 kHz, a pulse energy of 410 μJ and a square pulse $\sim$ of $\tau_1 = 715$ ns FWHM (average power of 5.75 W). The beam is collimated with a telescope lens with a diameter of 12 cm to reach great distances. The simulation was performed with a Gaussian time gate of $\tau_2 = 570$ ns FWHM. The simulated atmosphere corresponds to the cases described in Fig. 1 using constant wind and the measurements were integrated over 2 s. The standard deviation was determined using Monte Carlo simulations. In this configuration, the spatial resolution is given by $c(\tau_1 + \tau_2)/2 \approx 200$ m.

B. QMZ spectral analyzer for molecular scattering

The design of the field-compensated QMZ, that was first proposed by the LATMOS laboratory [21] has been detailed in several articles [22]. It consists in using a Mach-Zehnder interferometer where an optical path difference (OPD) is made between the two arms so that the phase of the interference at the exit of the interferometer depends on the frequency of the incoming light. A quarter-wave plate is inserted into one arm of the interferometer, and four polarizers at its output to separate the signal into four quadrature interference components ϕ - $\phi_0 = [0, \pi/2, \pi, 3\pi/2]$ where ϕ_0 corresponds to the phase shift between the two arms at the first output of the interferometer [Fig. 2c)]. In this case, we can show that the spectral shift of the interference pattern is proportional to the frequency of the light. Then, the frequency shift is deduced from the phase shift of the interference figure measured for the backscattered light and the laser light.

In order to describe the performance of such a lidar to measure wind in the atmosphere, we performed simulations of the QMZ lidar [Fig. 3 b)]. This development is performed within the framework of the European project Cleanaviation/Upwing [23]. The simulated lidar uses a 3 cm OPD adapted to measure the Rayleigh scattering of molecules. It uses a 351 μm pulsed laser at 400 Hz with pulse energies of 22.5 mJ which match the characteristics of the MERION C injected laser developed by Lumibird. The optical configuration is bistatic (different lenses are used to shape the laser and collect the signal) coaxial (same axis for transmission and reception). The laser is collimated

with a final lens of 2 cm in diameter. The receiver is made with a Newton telescope with a primary mirror of 15 cm in diameter. Measurements are averaged over 200 m that correspond to the spatial resolution. To compare results with the heterodyne lidar, the same instrumental configuration is used, i.e. the lidar is located on the ground and directed upwards. The simulations show a larger error before 2 km of altitude but much better performances after 2 km. Measurements can be made up to 20 km of altitude.

III. Specific developments to use lidar on-board

For many applications, it is interesting to embed a wind lidar on board an aircraft. This can be done in particular to help with aerial navigation, to perform wind measurements at high altitude bringing the lidar closer to the region of interest and thus obtaining better measurement accuracy, or to follow Aeolus measurement for calibration/validation application. However, to embed a lidar in an aircraft, dedicated developments are necessary. In particular, the lidar must be reinforced to handle the vibration conditions. It must also be reliable and potentially automated to use lidar remotely because the cost of flying by plane is significant and a limited number of people can be on board at the same time. It also needs to get fast measurements to integrate data over small distances despite the fast moving aircraft. In this chapter, we will detail the improvements made or under development to embed the two ONERA lidar architectures on aerial carriers. For heterodyne technology, many lidars have been used on board airplane at ONERA [5], [24], [25]. In this article, we will focus on the description of the LIVE lidar which has been successfully flown on board an ATR42 SAFIRE (Service des Avions Français Instrumentés pour la Recherche en Environnement). For molecular lidar technology with QMZ, we will describe the developments currently being carried out within the framework of the CleanAviation/Upwing project to embed the lidar on aircraft.

A. Heterodyne lidar

For the LIVE lidar, a robust laser architecture was developed with a fiber laser emitting at 1.5 μm followed by a fiber amplifier [Fig. 4a)]. It delivers gaussian pulses of length 715 ns FWHM allowing to reach a long distance. It also has a narrow spectral width (close to the limit by the Fourier transform) and a high beam quality factor ($M^2 = 1.1$) suitable for heterodyne detection. The latest fiber amplifier has a large core to reduce the Brillouin instability problem and thus improve the maximum power in the pulse (∼500 W) to reach a high energy per pulse of 410 μJ.

To manage the vibration conditions, a monostatic fibered transmission/reception design was carried out. To simplify the installation in aircraft, all the lidar elements were inserted into standard racks [Fig. 4b)]. An automated mechanical system was set up to perform a rotary scan of $\sim$ 17 s below the aircraft [Fig. 4c)] to measure the different components of the wind vectors and recover the 3-D wind vectors. A specific algorithm suitable for rotary scanning has been implemented

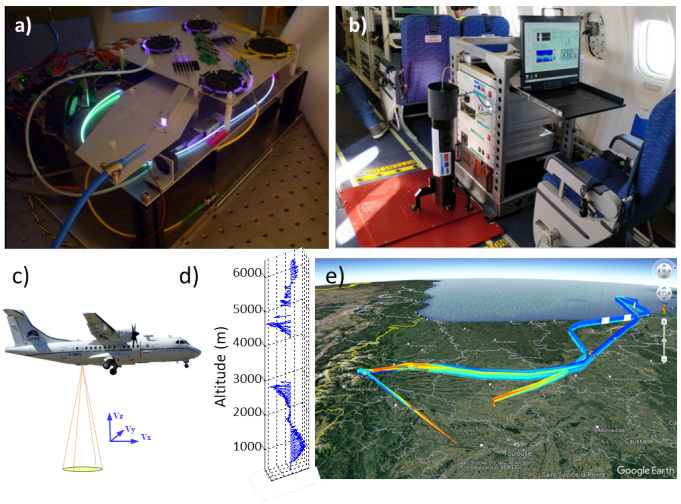

Fig. 4. Picture of the 1.5 μm fiber laser (a) and of the lidar integrated in airplane (b). c) schematic of the lidar in the airplane. d) Example of reconstructed wind profile. e) Evolution of the wind measurements during the flight.

[26] to perform analysis of the data. A man-machine interface was made to control all Lidar parameters.

Several campaigns were carried out in 2019 near the city of Fauga to measure the 3D wind profile. An example of wind reconstruction is shown in Fig. 4d). We see that the wind could be measured between the ground and 6.5 km altitude with measurements covering almost the entire axis. Fig. 4e) shows that the rapid motion of the aircraft was used to measure the wind profile over large areas. During the campaign, comparisons were made with measurements obtained with a WinCube lidar and showed that with the LIVE lidar, we obtain an accuracy on each of the three components of the wind vector better than 0.5 m/s with a horizontal resolution of 3 km and a vertical resolution of 100 m.

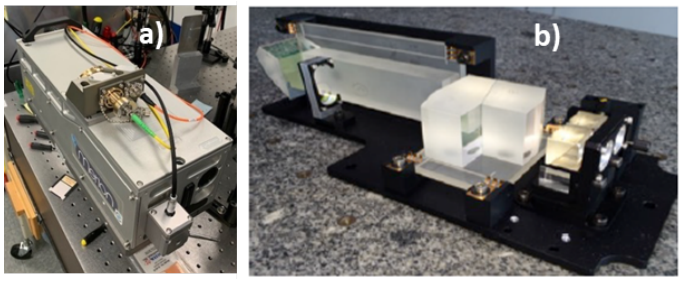

Fig. 5. a) Picture of the injected Merion C laser developed by Lumibird. b)Picture of the monobloc QMZ lidar développed by the LATMOS for the HSR-LNG

B. Direct detection QMZ lidar

For the QMZ lidar, a first laser solution was to purchase the injected solid laser developed by Lumibird called Merion C [Fig. 5a)]. It delivers 7 ns, 22.5 mJ, 351 nm laser pulses with a pulse repetition frequency of 400 Hz. It has a narrow spectral width (close to the limit due to the Fourier transform)

necessary for the measurement. Unlike the heterodyne solution, the constraint on the quality of the beam is less important ($M^2 = 5$). A second laser solution is also under development which is, like the heterodyne lidar, a fiber solution [27]. A simulation study was carried out to determine the optimized laser parameters (40 KHz and 25 ns per pulse) [28]. The fiber laser will have many advantages over the solid-state laser, including reduced cost, better vibration robustness, better compactness. This architecture may include free-space amplifiers to achieve higher energies per pulse. It can be noticed that the alignment is much less critical for free space amplifiers than for laser cavities. The architecture is then intrinsically more robust to vibrations.

The QMZ interferometer is built similarly to the HSR-LNG [29] with an assembly of prisms and plates to form a monolithic interferometer [Fig. 5b)]. Development is underway and will include a mechanical assembly that manages the vibration conditions encountered in aircraft. Additionally, a robust transmit/receive architecture is being developed and all parts will be racked as for heterodyne lidars.

IV. Potential applications for spatial agencies

In this part we discuss the potential applications for space agencies of the two wind lidar technologies developed at ONERA. We start discussing applications for AEOLUS calibration/validation campaigns. Then, we study the advantages that the developments made for the UV lidar could have for a future architecture of AEOLUS.

A. Calibration/validation of AEOLUS

Although heterodyne particle lidars do not work at high altitudes and at all times, they generally provide a much more accurate measurement of wind speed than molecular lidars [Fig. 3a)]. With a lidar on the ground, the simulations indicate that one can obtain a speed measurement with a standard deviation of less than 0.1 m/s up to 3.5 km altitude 50% of the time. In addition, the heterodyne lidar developed at ONERA can be used on board aircraft, which makes it possible to bring the lidar into the upper atmosphere to obtain more precise measurements at high altitude. This method was used during the live campaign to obtain measurements up to 6.5 km altitude: between 4 km and 6.5 km, the signal measured was strong because the measurement area was close to the lidar and between 0 km and 3 km the signal was strong because the density of the particles was important. In addition, an onboard lidar is useful for AEOLUS calibration/validation campaigns because it allows it to be positioned at the level of the satellite's measurement axis.

Simulations also indicate that the UV lidar architecture developed at ONERA should make it possible to measure wind speed up to 20 km altitude [Fig. 3b)]. The fact that this lidar should be on board an aircraft is interesting for a calibration/validation campaign in order to position the lidar next to the axis of the satellite.

B. Developments for future AEOLUS generation

The field-compensated QMZ lidar currently developed within an ONERA-LATMOS collaboration has many advantages detailed in [7] including a larger acceptance angle reducing mechanical and thermal stresses, the absence of bias induced by the scattering of aerosols on the Doppler shift, the possibility of determining the position of clouds and the quantity of aerosol and the establishment of a depolarized channel allowing the types of aerosol to be distinguished.

The use of the UV fiber laser could also be very beneficiary to get a cheaper, lighter, more compact and more robust laser solution for a future AEOLUS generation.

V. Conclusion

In summary, we present the two wind lidar architectures developed at ONERA: the heterodyne lidar which analyzes the backscattering of particles and the direct detection lidar using a QMZ which analyzes the backscattering of molecules. In both cases, solutions have been developed to be able to embark them on an airplane: fiber laser, robust receiver, robust general architecture. Both technologies could provide interesting comparative measurements for AEOLUS calibration/validation campaigns: the heterodyne configuration allows precise measurements on the lower part of the atmosphere while the QMZ configuration allows reaching up to at an altitude of 20 km. In addition, regarding the developments made for molecular lidar, the UV fiber laser and the monolithic QMZ receiver could be excellent solutions for the next generation of Aeolus to reduce costs, improve data quality and lidar durability.

References

[1] D. C. Soreide, R. K. Bogue, L. J. Ehernberger and H. R. Bagley, "Coherent lidar turbulence for gust load alleviation," Optical Instruments for Weather Forecasting, vol. 2832, pp. 61 – 75, 1996

[2] H. Fournier, P. Massioni, M. Tu Pham, L. Bako, R. Vernay and M. Colombo, "Robust Gust Load Alleviation of Flexible Aircraft Equipped with Lidar," Journal of Guidance, Control, and Dynamics, vol. 45, pp. 58-72, 2022

[3] D. Cavaliere, N. Fezans, D. Kiehn, D. Quero and Patrick Vrancken, "Gust Load Control Design Challenge Including Lidar Wind Measurements and Based on the Common Research Model," AIAA SCITECH 2022 Forum

[4] A. dos Reis, P. Vuillemin, D. Quero and C. Poussot-Vassal, "Observer-based gust load alleviation via reduced-order models," IFAC-PapersOnLine, vol. 55, pp. 25-30, 2022

[5] B. Augere, C. Besson, D. Fleury, D. Goular, C. Planchat and M. Valla, "1.5 μm lidar anemometer for true air speed, angle of sideslip, and angle of attack measurements on-board Piaggio P180 aircraft," Measurement Science and Technology, vol. 27, pp. 054002, 2016

[6] T. STRGANAC, "Wind study for high altitude platform design," 3rd Lighter-Than-Air Systems Technology Conference, 1979

[7] D. Bruneau and J. Pelon, "A new lidar design for operational atmospheric wind and cloud/aerosol survey from space," Atmospheric Measurement Techniques, vol. 14, pp. 4375–4402, 2021

[8] M. Rennie, A. Stoffelen, S. Khaykin, S. Osprey, C. Wright, T. Banyard, A. G. Straume, O. Reitebuch, I. Krisch, T. Parrinello, Tommaso and others, "Demonstrated Aeolus Benefits in Atmospheric Sciences," 2021 IEEE International Geoscience and Remote Sensing Symposium IGARSS, pp. 763–766, 2021

[9] B. Witschas, Benjamin, C. Lemmerz, A. Geiß, O. Lux, U. Marksteiner, S. Rahm, O. Reitebuch and F. Weiler, "First validation of Aeolus wind observations by airborne Doppler wind lidar measurements," Atmospheric Measurement Techniques, vol. 13, pp. 2381–2396, 2020

[10] K. M. Bedka, A. R. Nehrir, M. Kavaya, R. Barton-Grimley, M. Beaubien, B. Carroll, J. Collins, J. Cooney, G. D. Emmitt, S. Greco,and others, "Airborne lidar observations of wind, water vapor, and aerosol profiles during the NASA Aeolus calibration and validation (Cal/Val) test flight campaign," Atmospheric Measurement Techniques, vol. 14, pp. 4305–4334, 2021

[11] S. C. Tucker, "OAWL: A HIGH-HERITAGE US DOPPLER WIND LIDAR FOR NEXT-GENERATION SPACE-BASED WIND AND AEROSOL OBSERVATIONS," 35th Space Symposium, Colorado, 2018

[12] O. Lux, C. Lemmerz, F. Weiler, U. Marksteiner, B. Witschas, S. Rahm, A. Geiß, and O. Reitebuch, "Intercomparison of wind observations from the European Space Agency's Aeolus satellite mission and the ALADIN Airborne Demonstrator," Atmospheric Measurement Techniques, vol. 13, pp. 2075–2097, 2020

[13] M. Ratynski, S. Khaykin, A. Hauchecorne, R. Wing, J.-P. Cammas, Y. Hello and P. Keckhut, "Validation of Aeolus wind profiles using ground-based lidar and radiosonde observations at Réunion island and the Observatoire de Haute-Provence," Atmospheric Measurement Techniques, vol. 16, pp. 997–1016, 2023

[14] R. G. Beranek, J. W. Bilbro, D. E. Fitzjarrald, W. D. Jones, V. W. Keller and B. S. Perrine, "Laser Atmospheric Wind Sounder (LAWS)," Laser Applications in Meteorology and Earth and Atmospheric Remote Sensing, vol. 1062, pp. 234 – 248, 1989

[15] W. E. Baker, G. D. Emmitt, F. Robertson, R. M. Atlas, J. E. Molinari, D. A. Bowdle, J. Paegle, R. M. Hardesty, R. T. Menzies, T. N. Krishnamurti, R. A. Brown, M. J. Post, J. R. Anderson, A. C. Lorenc and J. McElroy, "Lidar-Measured Winds from Space: A Key Component for Weather and Climate Prediction," Bulletin of the American Meteorological Society, vol. 76, pp. 869 - 888, 1995

[16] A. Dabas, M. L. Denneulin, P. Flamant, C. Loth, A. Garnier and A. Dolfi-Bouteyre, "Correcting winds measured with a Rayleigh Doppler lidar from pressure and temperature effects," Tellus A: Dynamic Meteorology and Oceanography, vol. 60, pp. 206-215, 2008

[17] X. Zhai, U. Marksteiner, F. Weiler, C. Lemmerz, O. Lux, R. Witschas and O. Reitebuch, "Rayleigh wind retrieval for the ALADIN airborne demonstrator of the Aeolus mission using simulated response calibration," Atmospheric Measurement Techniques, vol. 13, pp. 445–465, 2020

[18] C. Souprayen, A. Garnier, A. Hertzog, A. Hauchecorne and J. Porteneuve, "Rayleigh–Mie Doppler wind lidar for atmospheric measurements. I. Instrumental setup, validation, and first climatological results and II. Mie scattering effect, theory, and calibration," Appl. Opt., vol. 38, pp. 2410–2421, 1999

[19] B. Witschas, C. Lemmerz, A. Geiß, O. Lux, U. Marksteiner, S. Rahm, O. Reitebuch and F. Weiler, "First validation of Aeolus wind observations by airborne Doppler wind lidar measurements," Atmospheric Measurement Techniques, vol. 13, pp. 2381–2396, 2020

[20] B. Augere, M. Valla, A. Durécu, A. Dolfi-Bouteyre, D. Goular, F. Gustave, C. Planchat, D. Fleury, T. Huet and C. Besson, "Three-Dimensional Wind Measurements with the Fibered Airborne Coherent Doppler Wind Lidar LIVE," Atmosphere, vol. 10, pp. 549, 2019

[21] D. Bruneau, "Mach–Zehnder interferometer as a spectral analyzer for molecular Doppler wind lidar," Applied Optics, vol. 40, pp. 391–399, 2001

[22] S. C. Tucker, C. S. Weimer, S. Baidar and R. M. Hardesty, "The optical autocovariance wind lidar. Part I: OAWL instrument development and demonstration," Journal of Atmospheric and Oceanic Technology, vol. 35, pp. 2079–2097, 2018

[23] @onlineAdress, url = https://cordis.europa.eu/project/id/101101974,

[24] J.-P. Cariou, B. Augere, D. Goular, J.-P. Schlotterbeck and X. Lacondamine, "All-fiber 1.5 μm CW coherent laser anemometer DALHEC. Helicopter flight test analysis 13th," 13th Coherent Laser Radar Conf. (Kamakura), 2005

[25] D. T. Michel, A. Dolfi-Bouteyre, D. Goular, B. Augère, C. Planchat, D. Fleury, L. Lombard, M. Valla, and C. Besson, "Onboard wake vortex localization with a coherent 1.5 μm Doppler LIDAR for aircraft in formation flight configuration," Optics Express, vol. 28, pp. 14374–14385, 2020

[26] I. Smalikho, "Techniques of wind vector estimation from data measured with a scanning coherent Doppler lidar," J. Atmos. Ocean. Technol., vol. 20, pp. 276–291, 2003,

[27] J. Pouillaude, P. Pichon, X. Delen, P. Georges et L. Lombard, "Amplification d'impulsions monofréquences et nanosecondes dans des fibres copées Yb courtes: 1030 nm ou 1064 nm?" Journée nationale d'optique guidée, 2023

[28] T. Boulant et al., to be published

[29] D. Bruneau, J. Pelon, F. Blouzon, J. Spatazza, P. Genau, G. Buchholtz, N. Amarouche, A. Abchiche and O. Aouji, "355-nm high spectral resolution airborne lidar LNG: system description and first results," Applied optics, vol. 54, pp. 8776–8785, 2015